ELSEVIER

Polymer Vol. 37 No. 1, pp. 85–91, 1996

0032-3861/96/$15.00+0.00

The crystallization behaviour and phase diagram of extended-chain crystals of poly(vinylidene fluoride) under high pressure

Takeshi Hattori, Masamichi Hikosaka* and Hiroji Ohigashi†
Department of Materials Science and Engineering, Faculty of Engineering, Yamagata University, Yonezawa 992, Japan
(Received 29 May 1995; revised 6 July 1995)

In order to obtain the pressure–temperature (P–T) phase diagram of poly(vinylidene fluoride) (PVDF), the melting and crystallization behaviours under high pressure were investigated as a function of temperature and pressure. A corrected P–T phase diagram, in which the triple point (orthorhombic, hexagonal and melt) exists at 320 MPa and 300°C, is proposed. A film mainly consisting of extended-chain lamellar crystals of β-form can be obtained by crystallization in the metastable hexagonal phase, which appears when increasing pressure is applied on the melt. This crystallization method provides good-quality β-form films without thermal degradation.

(Keywords: poly(vinylidene fluoride); extended-chain crystals; phase diagram)

INTRODUCTION

The strong piezoelectric activity and conspicuous ferroelectric phenomena in copolymers of vinylidene fluoride and trifluoroethylene, P(VDF-TrFE), with VDF content in the range of ca. 60–82 mol% are attributable to thick lamellar crystals of β form regarded as extended-chain crystals (ECCs), which grow only when the copolymers are annealed in the paraelectric phase, a disordered phase called the hexagonal phase or rotator phase[1–4]. In this phase the chain molecules undergo incoherent rotational motion around their chain axes[5], and slide very easily along the direction of the chain axes as a liquid crystal[6]. Lamellar thickening through the sliding diffusion[7–10] in the hexagonal phase results in extended-chain crystals.

Since the electromechanical coupling factor k_t is proportional to the remanent polarization P_r, copolymers with higher VDF content are expected to exhibit larger k_t (refs 1, 2). The maximum k_t value, which is evaluated semiempirically to be 0.37, may be realized in a single crystal of β-form poly(vinylidene fluoride), PVDF[11]. It is well known that PVDF crystallizes into non-piezoelectric α-phase crystals at ordinary pressures, and it can be transformed into the β-form by mechanical drawing. However, the k_t values of the β-form PVDF film thus prepared is only 0.2 at most[12], the value being too small compared to the expected maximum value of k_t because of low crystallinity. Moreover, the polarization in such a β-form film is thermally unstable; depolarization occurs at a temperature far below the melting point T_m and the Curie temperature T_c. This is because the β-form crystals in a mechanically stretched film are very tiny in size (about 10 nm thick) and include many conformational defects mainly consisting of GT sequences[4, 11].

It was first reported by Matsushige and Takemura[13, 14] and Matsushige *et al.*[15] that thick lamellar crystals of β form (β-ECCs), whose melting point is at 207°C, were grown in PVDF at high temperature and high pressure. Although many studies[13–22] on the high-pressure crystallization of PVDF have been carried out, the crystalline phase of PVDF at high pressures and high temperatures is not well understood. In a previous paper[16], we also reported that a PVDF film composed of thick lamellar β-form crystals, which are regarded as extended-chain crystals (ECCs), was obtained by crystallization in the hexagonal phase, which appears only at high pressures and high temperatures. In this paper, we proposed a P–T (pressure–temperature) phase diagram of the β-form PVDF based on the concept that the β-phase ECCs grow only in the hexagonal phase. Furthermore, we reported that high-pressure crystallized β-form PVDF film is useful as an ultrasonic transducer material usable at high temperatures[17]. However, its k_t value is much smaller than that expected, possibly because the crystallization is not complete and the poling condition is not adequate.

In order to realize a larger value of k_t in PVDF film, β-ECCs must grow more thoroughly in the film. Therefore, it is very important to find the crystallization conditions for better growth of β-ECCs. In the present paper, we propose a corrected P–T phase diagram of PVDF based both on high-pressure differential thermal analysis

* Present address: Faculty of Integrated Arts and Sciences, Hiroshima University, Higashihiroshima 724, Japan
† To whom correspondence should be addressed

(d.t.a.) and on the characterization of high-pressure crystallized films under various conditions. On searching for better crystallization conditions, it is very important to note that, since violent thermal degradation of PVDF occurs above 300°C, the hexagonal phase appearing below 300°C should be found.

EXPERIMENTAL

High-pressure crystallization was performed by two methods as follows: In the first method (constant-pressure method), the original α-form PVDF films (Kureha KF film) were first heated up to 200–300°C under a constant pressure (150–500 MPa) and then cooled below 100°C at a rate of about 1°C min^{-1} before releasing the pressure. In the second method (constant-temperature method or pressure quenching method), α-form films were first melted at a low pressure (initial pressure) and then the pressure was increased up to 500 MPa at a constant temperature. Silicone oil was used as a pressure transmission medium.

Samples A–G were treated by the constant-pressure method. The pressure and the maximum temperature experienced for A–G are: A, 282°C, 150 MPa; B, 277°C, 200 MPa, C, 277°C, 260 MPa; D, 287°C, 300 MPa; E, 287°C, 360 MPa; F, 287°C, 400 MPa; G, 300°C, 500 MPa.

Samples H–L were crystallized by the constant-temperature method. The melting temperature and the initial and final pressures experienced for each sample are: H, 217°C, 100 and 500 MPa; I, 232°C, 150 and 500 MPa; J, 242°C, 150 and 500 MPa; K, 262°C, 150 and 500 MPa; L, 282°C, 200 and 500 MPa.

Melting behaviour under high pressure was studied by differential thermal analysis (d.t.a.) at various pressures. Differential scanning calorimetry (d.s.c.), scanning electron microscopy (SEM), transmission electron microscopy (TEM), electron diffraction (ED), X-ray diffraction and polarized optical microscopy (POM) were employed to characterize the structure of high-pressure crystallized films.

RESULTS

D.s.c. thermograms

Figure 1a shows the typical d.s.c. thermograms recorded at 0.1 MPa for samples A–G. As shown later, samples A–E were once melted at high pressures, whereas samples F and G were annealed just below the melting point of the α-form. *Figure 1b* displays the d.s.c thermograms for samples H–L crystallized from the melt under successively increasing pressure at fixed temperatures.

The endothermic peaks of these samples occur at various temperatures between 173 and 206°C. The endotherms at 173–179°C are attributable to the melting of α crystals, while those at 203–206°C are assigned to the melting of β-ECCs. The endotherms at 182–196°C are attributable to the melting of crystallites, which may be assigned to folded-chain β crystals or γ-form crystals, as described later. These assignments are essentially similar to that reported by Matsushige *et al.*[13–15].

In samples A–E, the intensity of the endothermic peak around 175°C decreases whereas that around 203°C increases with increasing crystallization pressure. Similarly, in samples H–K, the area of the endothermic peak around 175°C also decreased while that around 205°C is not observed in samples F and G, which were not heated above the melting point of the α phase and did not pass through the hexagonal phase as described later.

X-ray diffraction profiles

Figure 2 shows the X-ray diffraction profiles of the samples A, D, F, H and K. Referring to the X-ray diffraction data[20,23,24] these reflection peaks are characterized as follows: the reflections at 17.8° and 18.4° are assigned to 100α and 020α (the 100 and 120 reflections of the α phase, respectively); 20.2° to 110α or 100γ; 21.0° to $110\beta + 200\beta$ or 021γ; 26.6° to 021α; 35.2° to 001β or 131γ; 36.3° to 200γ; 39.4° to $132\gamma + 201\gamma + 041\gamma$; and 41.3° to 400β or $042\gamma + 221\gamma$.

Sample A is suggested to have a polar α-form or δ-form structure[23], because the intensities of the 020, 110 and 021 reflections of the α-form are strong, while the intensity of the 100 (17.8°) reflection of the α-forms is very weak. In profile D, the strong reflections of β phase or γ phase are observed. In the samples crystallized from the melt during cooling under fixed pressure, the amount of α phase decreases while that of β phase and γ phase increases with increase in crystallization pressure as mentioned before.

Sample F, which has endothermic peaks at 174°C (weak), 182°C (weak) and 192°C (strong), as shown in *Figure 1a*, exhibits X-ray diffraction from a mixture of β and γ phases. Therefore, the endotherms at 182–196°C on d.s.c. thermograms are due to the melting of the mixed structure of β phase and γ phase. Profile H has reflections from all phases, i.e. α, β and γ phases.

In profile K, reflections of the α phase disappear, and reflections of γ phase decrease in intensity compared to profile H. In the samples crystallized from the melt under a successively increased pressure at fixed temperature, the amount of α phase and γ phase decreases whereas that of β phase increases with increase in crystallization temperature.

POM, SEM and TEM images

Figure 3 shows the polarized optical micrographs of samples A, D, H and K. Typical α-form spherulitic crystals are observed throughout A, and those embedded in a dark background are observed in H, β-ECCs, which exhibit cigar-shaped morphology due to their edge-on orientation in the films, are observed in D and K. Although sample K is filled with β-ECCs, cigar-shaped morphology is not clear. In sample D, spherulitic crystals and darker areas are observed around β-ECCs. The endotherms at 182–196°C on d.s.c. thermograms are considered to be due to melting of the crystals, which look darker in the POM image. The darker area is composed of very tiny lamellar crystals, which have mixed structure of β phase and γ phase.

In *Figures 4a* and *4b* are shown the SEM images of sample K and sample G, respectively. Thick lamellar crystals about 0.1 μm thick are observed all over the fractured cross-section of sample K, while very tiny lamellar crystals are observed in sample G. The TEM images and the ED pattern, observed at an acceleration voltage of 200 kV, of the lamellar crystals developed in sample K are shown in *Figure 5*. (The TEM sample was

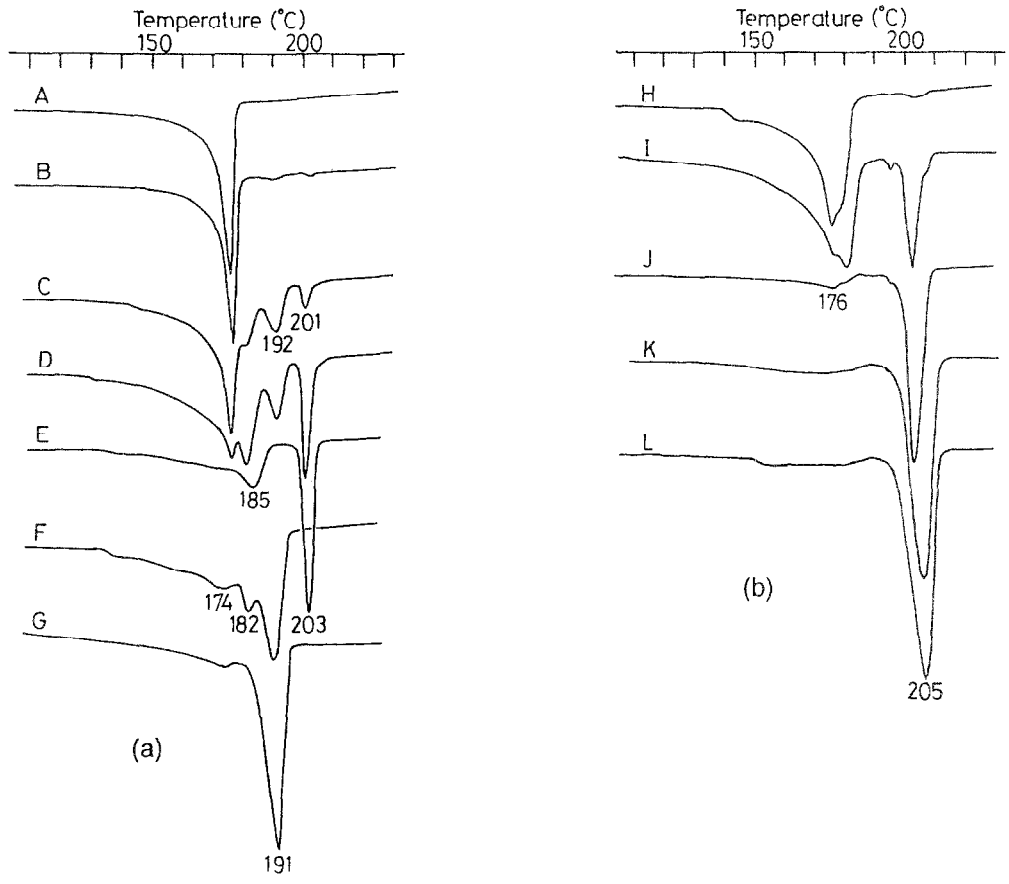

Figure 1. D.s.c. thermograms recorded at atmospheric pressure for PVDF films prepared by (a) the constant-pressure method (A–G) and (b) the constant-temperature method (H–L). (a) The pressure and the maximum temperature experienced for A–G are: A, 282°C, 150 MPa; B, 277°C, 200 MPa; C, 277°C, 260 MPa; D, 287°C, 300 MPa; E, 287°C, 360 MPa; F, 287°C, 400 MPa; and G, 300°C, 500 MPa. (b) The melting temperature, and the initial and final pressures experienced for H–L are: H, 217°C, 100 → 500 MPa; I, 232°C, 150 → 500 MPa; J, 242°C, 150 → 500 MPa; K, 262°C, 150 → 500 MPa; and L, 282°C, 200 → 500 MPa

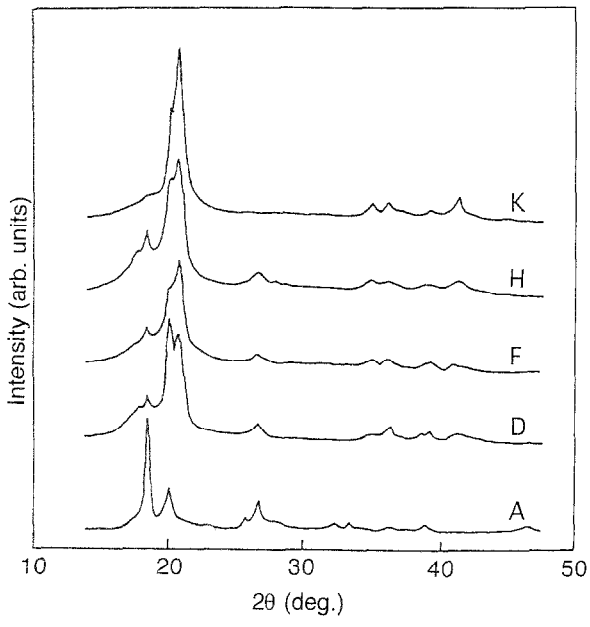

Figure 2 X-ray diffraction profiles of high-pressure crystallized PVDF (samples A, D, F, H and K)

prepared by grinding the sample K in liquid nitrogen.) The pattern, which consists of diffraction spots arranged approximately in hexagonal symmetry, is quite similar to those observed in P(VDF-TrFE) with VDF content in the range of ca. 60–88 mol%[3,4]. The *d*-spacing of the (110) or (200) planes determined from the pattern is 4.25 Å, which is consistent with that determined from X-ray diffraction and is 5–7% smaller than that of P(VDF-TrFE) copolymers of composition 79/21 or 75/25 mol%[2,3]. Even though the object of the TEM image comprises several sheets of stacked lamellae, its ED pattern looks like that from a single crystal. This indicates that one lamella stacks on another aligning their crystal axes in the common directions, in similar fashion as reported for the copolymers with VDF content ca. 60–88 mol%[3,4]. Therefore, we may infer that the lamellar crystal of PVDF grows epitaxially on the adjacent lamella, and that the 'regular re-entry model' is more reasonable to describe the folding of chain molecules at the lamellar surface; loose loops re-entering randomly into the same lamella, free chain ends (cilia), or tie molecules connecting adjacent lamellar crystals hardly exist in the region between lamellar crystals.

High-pressure d.t.a. thermograms

Figure 6 shows the high-pressure d.t.a thermograms, recorded at 0.1, 200 and 340 MPa in the heating process at a heating rate of 5°C min^{-1}, of the PVDF film composed of β-ECCs. The samples used in this experiment were prepared by high-pressure crystallization under the following conditions: molten at 250°C and

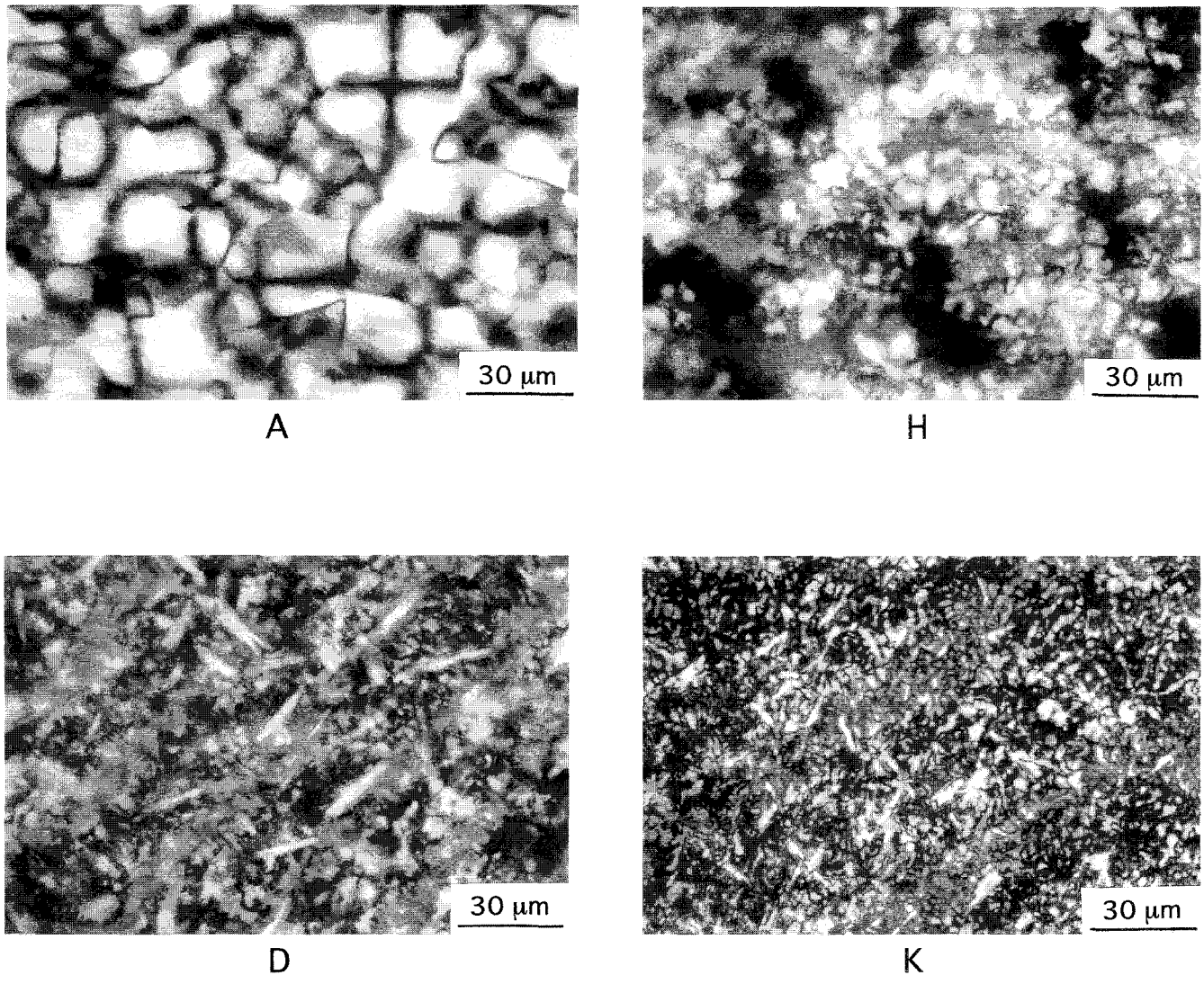

Figure 3 Polarized optical micrographs of high-pressure crystallized PVDF (samples A, D, H and K)

150 MPa, then crystallized by increasing pressure up to 500 MPa at 250°C and then cooled down to 50°C. The single endothermic peak corresponding to the melting of β-ECCs occurs at 205°C under 0.1 MPa, and shifts to higher temperature with increasing pressure. Since d.t.a. measurement above 350 MPa is difficult owing to intensive thermal degradation, we have not succeeded in observing the Curie temperature T_c (phase transition from ferroelectic or orthorhombic phase to paraelectric or hexagonal phase) separate from the melting point

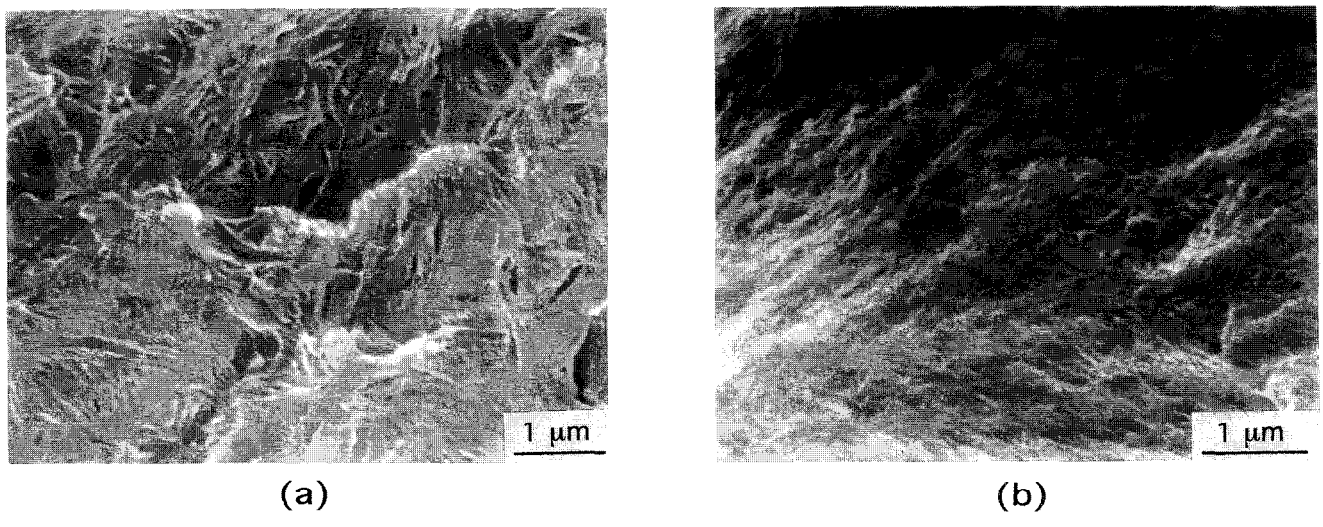

Figure 4 SEM images of PVDF: (a) thick lamellar β-form crystals of PVDF grown in sample K; (b) tiny lamellar crystals grown in sample G

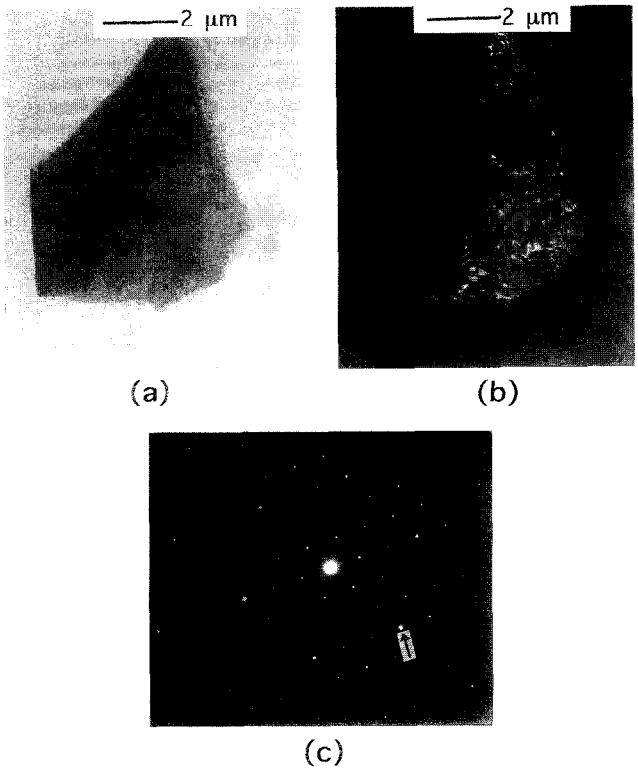

Figure 5 A stack of several sheets of lamellar single crystals (β form) grown in sample K: (a) bright-field and (b) dark-field TEM images, and (c) electron diffraction pattern. The dark-field image is observed by the 330 or 600 reflection marked with an arrow

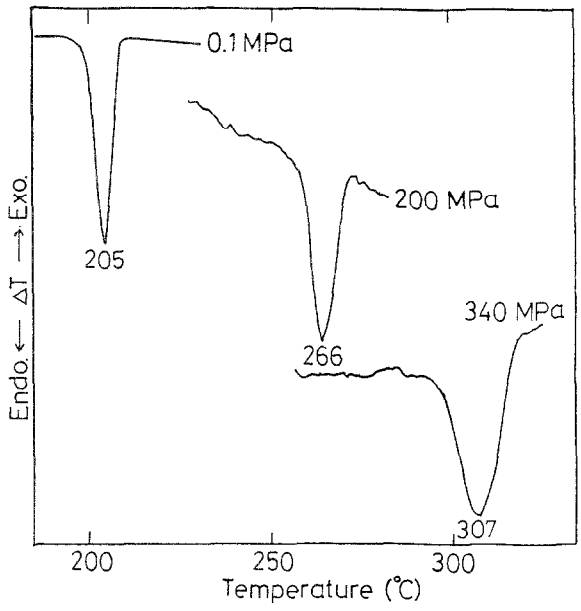

Figure 6 D.t.a. thermograms, recorded at 0.1, 200 and 340 MPa in the heating process at a heating rate of 5°C min^{-1}, of the PVDF film composed of thick lamellar β-form crystals

T_m(h) (from hexagonal phase to liquid phase). However, the endothermic peak observed under 340 MPa is much wider than that obtained under 200 MPa as shown in *Figure 6*. This suggests that the T_c and T_m(h) peaks begin to separate slightly at a pressure just below 340 MPa. Therefore, it is reasonable that the triple point exists near 320 MPa and 300°C. T_c and T_m(h) are expected to be observed as isolated endothermic peaks at pressures higher than 350 MPa if more thermally stable PVDF is available.

DISCUSSION

P–T *phase diagram*

The P–T phase diagram for PVDF is of utmost importance in high-pressure crystallization of PVDF. In a previous paper[16], we proposed a P–T phase diagram based on high-pressure d.t.a. and the assumption that thick lamellar crystals of PVDF are only developed in the hexagonal phase or paraelectric phase appearing at high pressure. However, the P–T phase diagram in that paper includes some uncertainties. At the present stage, we can propose a more definite P–T phase diagram based on the knowledge accumulated presently. As described in the preceding section, the triple point of orthorhombic, hexagonal (paraelectic) and liquid phase appears around 320 MPa at 300°C. The melting point of hexagonal phase T_m(h) and the phase transition temperature T_c above the triple point cannot be measured experimentally because of the explosive thermal degradation of PVDF. Therefore we predict them from dT_m/dP and dT_c/dP, which have been obtained for P(VDF-TrFE), where P represents pressure.

In previous papers[4,16,17,25], we showed that the β-ECCs with VDF content higher than 82 mol%, which are prepared by high-pressure crystallization or by field-induced phase transformation of thick lamellar crystals composed of α, γ and β phases, exhibit only a single endothermic peak in d.s.c. thermograms as a melting point. This peak splits into two peaks at high pressures, the low-temperature peak corresponding to Curie temperature T_c and the high-temperature peak corresponding to the melting point of the hexagonal phase T_m(h)[17,25].

In *Figure 7* the values of dT_c/dP and $dT_m(h)/dP$, which are obtained from d.t.a. data for P(VDF-TrFE) copolymers, are plotted as a function of VDF content. Extrapolating these rates of VDF 100% (PVDF), dT_c/dP and $dT_m(h)/dP$ are estimated to be 19 K/100 MPa and 37 K/100 MPa, respectively. Using these values, we have a new P–T phase diagram for PVDF. This is shown in *Figure 8*. Below the triple point, the T_m *versus* P relationship is plotted using the data of the high-pressure d.t.a. obtained for β-ECCs. In *Figure 8*, the melting point of α-phase crystals of PVDF $T_m(\alpha)$ is also plotted.

Metastable hexagonal phase

β-ECCs are grown in the paraelectric (hexagonal) phase above the Curie point T_c. However, the stable hexagonal phase of PVDF exists at temperatures and pressures so high that thermal degradation of PVDF easily occurs during crystallization in the hexagonal phase. Fortunately, for PVDF initially in the liquid state, the hexagonal phase appears below the triple point as a metastable state. In *Figure 9* samples A–L are put on the P–T phase diagram according to their crystallization conditions. In this figure, T_s(h) indicates the crystallization temperature of β-ECCs in cooling at a rate of 1°C min^{-1}, and T_s(o) indicates the crystallization temperature of orthorhombic phase in increasing pressure at a rate of 150 MPa min^{-1}. T_s(h) and T_s(o) depend on the rate of cooling or increasing pressure. As seen in *Figure 9*, β-ECCs of PVDF in samples C–E and I–L are those that developed in the metastable hexagonal phase. When α-form films were first melted at 0.1 MPa and

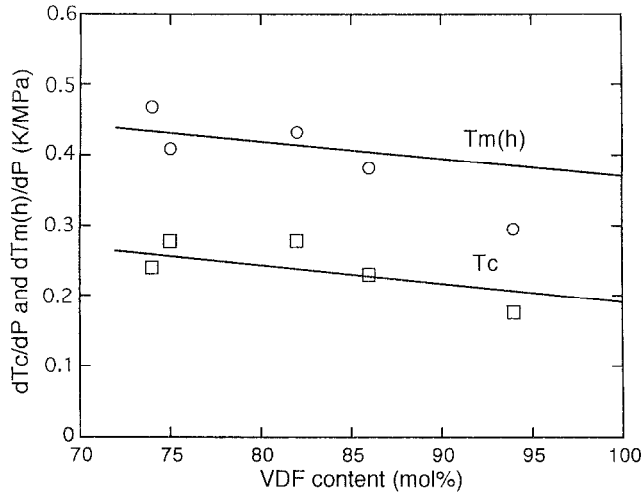

Figure 7 Plots of dT_c/dP and $dT_m(h)/dP$ of P(VDF-TrFE) as functions of VDF content. The data were obtained from high-pressure d.t.a.

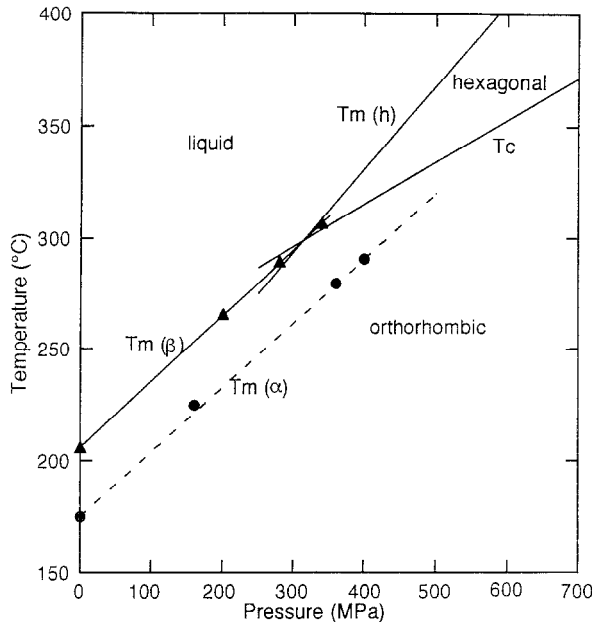

Figure 8 The P–T phase diagram for thick lamellar β-form crystals of PVDF. The melting curve for α-form $T_m(\alpha)$ is added (broken line) in the figure

222°C and then pressure was increased up to 200 MPa (sample M), 300 MPa (sample N) and 400 MPa (sample O) at 222°C, the resulting films M, N and O showed d.s.c. thermograms and optical morphology very similar to those of samples B, E and I, respectively. The hatched region in *Figure 9* shows the condition where thick lamellar β-form crystals grow very well without thermal degradation.

The high-pressure crystallization of PVDF below the triple point is similar to the crystallization of P(VDF-TrFE) copolymers with VDF 82–90 mol% from the melt at atmospheric pressure[4]: the metastable state appears also in these copolymers, and this phase plays an important role in the growth of thick lamellar crystals[4, 26]. (In the case of P(VDF-TrFE) with 82-90 mol% VDF, the metastable hexagonal phase also emerges directly from the mixed phase of β, γ and α phases without melting[4].)

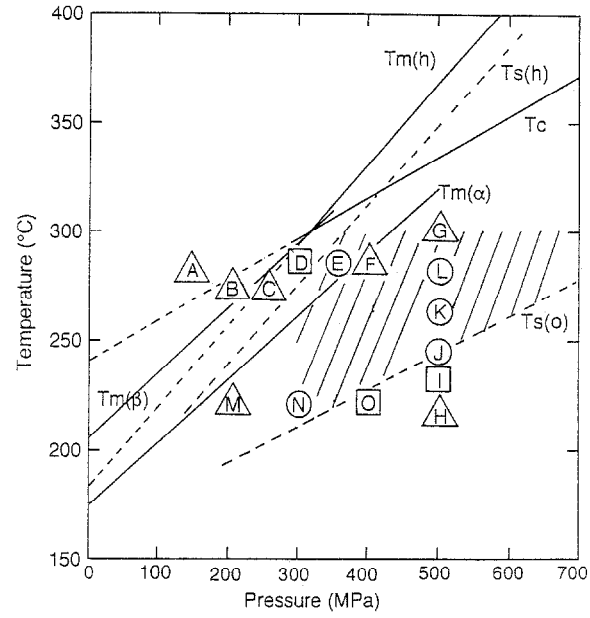

Figure 9 The plots of samples A–L on the P–T phase diagram according to their crystallization conditions. Symbols ○, □ and △ represent the samples in which thick lamellar β-form crystals grow very well, fairly well and very poorly, respectively

Since the metastable hexagonal phase in PVDF appears only from the liquid state, thick lamellar crystals do not develop in the film without melting at high pressure. This is the case of sample F (295°C, 400 MPa) and sample G (300°C, 500 MPa). Hasegawa *et al.*[19] heated PVDF up to 285°C at 400 MPa. In their experiment β-ECCs did not develop for the same reason. The β-ECC did develop in the PVDF heated up to 300°C at 400 MPa by Matsushige *et al.*[14–16], because the PVDF was melted and crystallized in the metastable hexagonal phase. Doll and Lando[18] and Scheinbeim *et al.*[21] obtained high-pressure crystallized PVDF having a melting point of 187–190°C. Considering that their starting material ('Kynar' α-form PVDF from Pennwalt Corp.) has a melting point of 160°C, about 15 K lower than the α-form PVDF used in our study ('KF' film from Kureha Chem. Industry Corp.), the high-pressure crystallized PVDF obtained in their study is probably β-ECCs. Iwamoto *et al.*[22] reported that extended-chain crystals of γ and γ' forms were grown by pressure quenching from 100 MPa to 600 MPa at 240°C. However, their assignment of the crystal form is ambiguous.

PVDF in metastable hexagonal phase transforms more quickly to orthorhombic phase for larger ΔT(oh) and the growth rate of β-ECCs is small for small ΔT(h) at lower pressure, where ΔT(oh) is the difference between T_c and T_s (crystallization temperature) and ΔT(h) is the difference between $T_m(h)$ and T_s. Therefore, β-ECCs are found to be more difficult to grow at lower pressure ($P < 300$ MPa) from the melt under a fixed pressure. On the other hand, PVDF in metastable hexagonal phase transforms more slowly to orthorhombic phase for small ΔT(oh), and the growth rate of β-ECCs is larger for large ΔT(h) in metastable hexagonal phase at higher pressure ($P > 300$ MPa). Therefore, as shown in *Figure 3*, sample K is filled with β-ECCs. However, the PVDF in metastable hexagonal phase transforms more quickly to orthorhombic phase for large ΔT(oh) at lower

temperature ($T < 250°C$) at 500 MPa. This is the reason why β-ECCs grown in sample J are tiny in size. β-ECCs hardly grow in sample H, indicating that this sample did not pass through the metastable hexagonal phase.

The poled film of the high-pressure crystallized PVDF composed of β-ECCs such as sample K was found to have strong piezoelectricity and large electromechanical coupling factor k_t of about 0.27, the largest value ever realized in PVDF. The piezoelectricity was found to be stable even at 200°C[7]. The piezoelectricity and related properties of high-pressure crystallized PVDF will be reported elsewhere[27].

CONCLUSIONS

We proposed a new P–T phase diagram of PVDF based on the high-pressure d.t.a. thermograms, knowledge obtained from high-pressure crystallization experiments and the concept that β-ECCs grow in a hexagonal phase or in the metastable hexagonal phase. We found the crystallization conditions for better growth of β-ECCs with minimal thermal degradation: PVDF is crystallized in metastable hexagonal phase by the constant-temperature method or pressure quenching method: α-form films were first melted at 100–200 MPa and 240–300°C and then pressure was increased up to 500–600 MPa at constant temperature.

ACKNOWLEDGEMENTS

We are grateful to Mr M. Kanaoka for his assistance in the experiments and M. Konno for preparation of experimental apparatus. This work was supported in part by Grants-in-Aid (No. 04555212 and No. 06452342) for Scientific Research from the Ministry of Education, Science and Culture, Japan.

REFERENCES

1 Ohigashi, H. and Koga, K. *Jpn. J. Appl. Phys.* 1982, **21**, L445
2 Koga, K. and Ohigashi, H. *J. Appl. Phys.* 1986, **59**, 2142
3 Ohigashi, H., Akama, S. and Koga, K. *Jpn. J. Appl. Phys.* 1988, **27**, 2144
4 Koga, K., Nakano, N., Hattori, T. and Ohigashi, H. *J. Appl. Phys.* 1990, **67**, 965
5 Tashiro, K., Takano, K., Kobayashi, M., Chatani, Y. and Tadokoro, H. *Ferroelectrics* 1984, **75**, 297
6 Ohigashi, H. and Saijio, T., Preprints, 4th SPSJ Int. Polym. Conf. 1992, p. 363
7 Hikosaka, M., Sakurai, K., Ohigashi, H. and Koizumi, T. *Jpn. J. Appl. Phys.* 1993, **32**, 2029
8 Hikosaka, M., Sakurai, K., Ohigashi, H. and Koizumi, T. *Jpn. J. Appl. Phys.* 1993, **32**, 2780
9 Hikosaka, M. *Polymer* 1987, **28**, 1257
10 Hikosaka, M. *Polymer* 1990, **30**, 459
11 Ohigashi, H., Proc. 6th Int. Meeting on Ferroelectricity, Kobe 1985, *Jpn. J. Appl. Phys.* 1985, **24**, *Suppl.* **24-2**, 23
12 Ohigashi, H. *J. Appl. Phys.* 1976, **47**, 949
13 Matsushige, K. and Takemura, T. *J. Polym. Sci., Polym. Phys. Edn.* 1978, **16**, 921
14 Matsushige, K. and Takemura, T. *J. Crystal Growth* 1980, **48**, 343
15 Matsushige, K., Nagata, K. and Takemura, T. *Jpn. J. Appl. Phys.* 1978, **17**, 467
16 Ohigashi, H. and Hattori, T. *Jpn. J. Appl. Phys.* 1989, **28**, L357
17 Ohigashi, H., Watanabe, T., Li, G. R., Hattori, T. and Takahashi, S. *Jpn. J. Appl. Phys.* 1989, **31**, *Suppl.* **31-1**, 111
18 Doll, W. W. and Lando, J. B. *J. Macromol. Sci., Phys. (B)* 1970, **2**, 889
19 Hasegawa, R. Kobayashi, M. and Tadokoro, H. *Polym. J.* 1972, **3**, 591
20 Hasegawa, R. Kobayashi, M. and Tadokoro, H. *Polym. J.* 1972, **3**, 600
21 Scheinbeim, J., Nakafuku, C., Newman, B. A. and Pae, K. D. *J. Appl. Phys.* 1979, **50**, 4399
22 Iwamoto, T., Itoh, T., Ando, Y., Miyata, S. and Konishi, K. *Jpn. J. Appl. Phys.* 1988, **27**, L1969
23 Davis, G. T., Mckinney, J. E., Broadhurst, M. G. and Roth, S. C. *J. Appl. Phys.* 1978, **49**, 4998
24 Weinhold, S., Litt, M. H. and Lando, J. B. *Macromolecures* 1980, **13**, 1178
25 Nakanishi, T., Ohigashi, H. and Minomura, S. *Rep. Prog. Polym. Phys. Jpn.* 1982, **25**, 509
26 Hikosaka, M., Sakurai, K., Ohigashi, H. and Keller, A. *Jpn. J. Appl. Phys.* 1994, **33**, 214
27 Hattori, T., Kanaoka, M. and Ohigashi, H. *J. Appl. Phys.* in press